PAPER • **OPEN ACCESS**

Operational domain estimation of a gamma-ray spectrometer for deuterium–tritium fusion power measurement at ITER

To cite this article: Giulia Marcer *et al* 2026 *Plasma Phys. Control. Fusion* **68** 055032

Plasma Physics and Controlled Fusion

OPEN ACCESS

RECEIVED
12 September 2025

REVISED
8 April 2026

ACCEPTED FOR PUBLICATION
11 May 2026

PUBLISHED
26 May 2026

PAPER

Operational domain estimation of a gamma-ray spectrometer for deuterium–tritium fusion power measurement at ITER

Giulia Marcer[1,*], Federico Scioscioli[1], Gabriele Croci[1,2], Andrea Dal Molin[1], Giuseppe Gorini[1,2], Andrea Muraro[1], Massimo Nocente[1,2], Enrico Perelli Cippo[1], Marica Rebai[1], Davide Rigamonti[1], Bruno Coriton[3], Andrei Kovalev[3], Alexei Polevoi[3] and Marco Tardocchi[1]

[1] Institute for Plasma Science and Technology, CNR, Milan, Italy
[2] Department of Physics, University of Milan-Bicocca, Milan, Italy
[3] Diagnostic Program, ITER Organization, Saint Paul-lez-Durance, France
[*] Author to whom any correspondence should be addressed.

E-mail: giulia.marcer@istp.cnr.it

Keywords: gamma-ray spectroscopy, tokamak, joint European torus, ITER, dynamic range

Abstract

ITER will be equipped with two types of diagnostics for fusion power measurement in deuterium–tritium plasmas: neutron flux monitors and neutron cameras, both absolutely counting the 14 MeV neutrons emitted by the D(T, ^{4}He)n reaction. The radial gamma-ray spectrometer (RGRS), though, has recently been considered as an additional fusion power diagnostic, detecting 17 MeV gamma-rays emitted by the radiative D(T, ^{5}He)γ channel of the DT reaction. This work describes the RGRS performance by determining the upper limit of its operational domain, strictly correlated with the expected background intensity and resulting between $2.6 \cdot 10^{17}$ neutrons per second and $3.2 \cdot 10^{18}$ neutrons per second. Based on this assessment, design optimization are introduced to fit the RGRS performances to the ITER requirements for safety-relevant fusion power measurements, for which the required operational range is between $2.4 \cdot 10^{19}$ neutrons per second and $3.2 \cdot 10^{20}$ neutrons per second. The expected different energy ranges covered by signal and background are exploited with the employment of a proper gamma-ray attenuator, allowing to widen and shift the RGRS operational domain toward the most relevant, high power plasma scenarios.

1. Introduction

Nuclear fusion is a promising source of clean energy. Recent experimental results and ongoing projects suggest that fusion power plants could start supplying electricity to the grid in the coming decades. As fusion moves from research to energy production, diagnostics measuring fusion power become crucial for assessing the reactor performances. The experimental tokamak ITER [1], currently under construction in southern France, will play a central role in this technological milestone.

Fusion power plants based on tokamak design will operate with deuterium–tritium (DT) as fuel, being the most promising reactants. Currently, though, only one direct method is available to measure fusion power in DT plasmas. This method relies on counting the neutrons produced in the DT fusion reactions, which are directly correlated with the generated power. However, additional independent methods would be valuable to cross-validate the experimental results and improve accuracy, thus enabling more efficient operation of future power plants.

The fission chambers which constitute the neutron flux monitors, although being the most accurate neutron yield measurement technique for time-resolved fusion power measurements at ITER, features a number of drawbacks. These diagnostics cannot distinguish between direct and scattered neutrons and

must therefore be calibrated in-situ or cross-calibrated using the neutron activation system [2–5]. In-vessel calibration is time-consuming and relies on complex, computationally intensive simulations of the entire tokamak environment. In addition, any change in the reactor configuration requires a new calibration. In light of these challenges, the implementation of a second, independent method for measuring fusion power is increasingly justified.

A novel, neutron-independent, direct method to measure fusion power was developed at the joint European torus (JET). This technique was demonstrated during the JET second DT experimental campaign (DTE2) [6–9]. To develop this technique, an absolutely calibrated, large (3×6 inches) lanthanum bromide gamma-ray spectrometer, already installed along a tangential line of sight (LoS), was employed [10]. This system was used to detect the high energy ($\sim$17 MeV) gamma-rays emitted by the D(T,^{5}He)γ reaction, the less probable secondary branch of the DT fusion process, which features a small branching ratio of barely $2.4(5) \cdot 10^{-5}$ [7]. A 90 cm long cylinder of LiH attenuator [11, 12] was used to attenuate the 10^5 times more intense neutron background. The DT gamma-ray signal was extracted from the spectra and scaled to the fusion power using a dedicated algorithm that accounts for the spatial distribution of the plasma emission [6]. In these studies, this spatial information was derived from the JET neutron camera.

The main drawback of this novel method is represented by an intense background which covers the low energy range of the spectrum up to about 9 MeV. At JET, this background was 10^3 times for intense than the signal and mostly caused by prompt gamma-rays generated by neutron capture on the surface of the tokamak inner vessel or central column, in the areas intercepted by the detector cone of sight [13]. The spectroscopic capabilities of the gamma-ray detector were used to separate the signal from the background.

Compared to the standard neutron-based diagnostics, this novel technique offers several advantages. First, lanthanum bromide scintillators can be absolutely calibrated in both energy and efficiency using their intrinsic radioactivity [14]. Second, gamma-ray interactions with matter are simpler and the cross sections are known with better accuracy than those of neutron interactions. Third, unlike fission chambers and activation foils, the signal can be distinguished from the background by leveraging the detector spectroscopic capabilities. As a result, the method does not require an in-vessel calibration or extensive Monte Carlo simulations. Moreover, the background is generated only inside the detector cone of sight, which limits the region of interest to a small part of the whole tokamak environment, making the detector calibration independent to the rest of the tokamak geometry, making it unnecessary to repeat the calibrations after any change in the reactor configuration.

Among other systems, ITER will also feature the radial gamma-ray spectrometer (RGRS) [16], a diagnostic primarily designed to provide measurements of the runaway electron distribution and the spatial profile of alpha particle density. The RGRS will consist of four detectors, with three of them observing the plasma through three dedicated, radial, coplanar, collimated LoSs, positioned approximately 18 m from the torus center. The fourth detector was not taken into account for this study, being it shared with other diagnostics while featuring a smaller LoS diameter, which prevented its application for fusion power measurements. All three LoSs observe portions of plasma above the equatorial plane ($z = 0$) as shown in figure 1. Each detector will comprise a 3×3 inches cylindrical scintillating lanthanum bromide crystal coupled to a photomultiplier tube. In front of it, 120 cm of LiH neutron attenuator will attenuate the direct neutron flux.

ITER has two types of fusion power measurement requirements: one for basic control, requiring high-speed (1 ms time resolution) and high-accuracy diagnostics, and an other for machine protection, with a less stringent time resolution required (1 s), limited to full power plasma scenarios. Recently, it has been shown that it is possible to use the RGRS to perform fusion power measurements at ITER while satisfying the safety requirements. The developed solution leverages the LoSs plurality of the diagnostic to improve the fusion power measurement accuracy and make it independent of external information of the plasma spatial distribution [14, 17] or just relying on additional magnetic equilibrium information [18]. Based on the required time resolution of 1 s, these works showed that the developed technique would allow to achieve the required accuracy (below 10%) above $2.6 \cdot 10^{17}$ neutrons per second (n s^{-1}), which is a lower neutron rate compared to the requested 10^{18} n s^{-1} lower limit.

As already mentioned, at JET, the majority of the events detected with the gamma-ray spectrometer was background, energetically located mostly below 9 MeV (make reference to figure 3 of [8] as an example of acquired spectrum). This background mainly originated from prompt gamma-rays produced by neutron interactions with the inner vessel components. Several efforts were made to understand the origin of this background [13] but, due to the limited knowledge of the neutron interactions cross sections, it was not possible to reproduce in the simulations the measured background structures

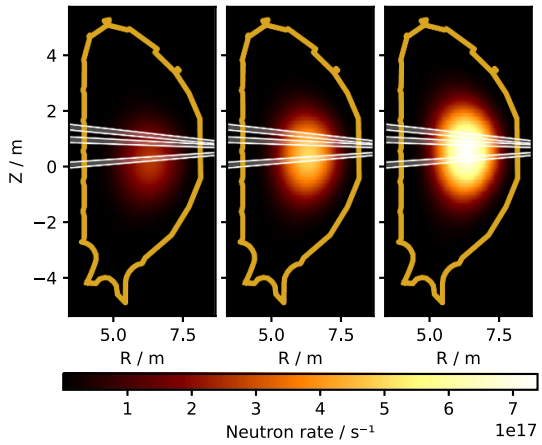

Figure 1. RGRS lines of sight inside the ITER vessel during the ramp-up of a full-power scenario. Emission profiles taken from integrated modelling and analysis suite (IMAS) [15], increasing time from left to right. The RGRS three LoSs are shown as three white, filled lines, while the vessel walls profile is shown in orange. Detectors are numbered from 1 to 3 starting from the lowest LoS.

quantitatively. Therefore, at present, this background cannot be used as an additional method for fusion-power measurements. Ongoing work aims to quantify the background observed at JET and exploit its direct correlation with fusion power to enable an independent measurement. Its intensity would support substantially higher time-resolution in fusion-power diagnostics.

When dealing with such high fluxes like those expected at ITER (about $10^8\,\mathrm{n\,s^{-1}}\cdot\mathrm{cm}^2$ in the 500 MW full power scenario), a very intense prompt gamma-ray background at the detectors is expected. Employing scintillation crystals coupled to photomultiplier tubes with such high neutron fluxes would entail to deal with a possible degradation of the signal due to pile-up [19–22] and digitalization paralysis. This defines an upper limit on the detector operational domain dictated by a too intense background which must be quantified. Since for the moment a background quantitative description is not available, this work focuses on the development of an alternative solution. This approach is based on the extrapolation from the background observed at JET at its RGRS during the DTE2. This work completes the studies previously reported in [17, 18] about the RGRS operational domain, providing the missing operational domain upper limit in terms of plasma total DT neutron rate.

The manuscript is organized as follows: the method adopted to quantify the expected background is described in details in section 2, followed by the achieved results in section 3; discussion and conclusions are given in sections 4 and 5.

2. Method

The upper limit of the operational domain is determined by the highest counting rate sustainable by the RGRS $LaBr_3$-based spectrometers. Based on JET experience, the pile-up starts affecting the collected spectra in an unrecoverable way as soon as the count rate reaches about 500 kHz [14]. $LaBr_3$ crystals represent the state of the art for gamma-rays measurements in tokamak environments. Therefore, at the moment this limit can not be improved and the neutron rate corresponding to 500 kHz event rate at each RGRS detector is to be determined.

Regardless of the reactor geometry and the detector at stake, the backbone of this method is the direct correlation between the plasma total neutron rate and the background count rate at the detector. Based on simulations and the experiments at JET, we assume that each count in the spectrum corresponds to one out of two possible events: a prompt gamma-ray generated at the tokamak walls or a direct neutron. Being 10^5 times less intense, direct gamma-rays generated in the plasma (DT signal, Bremsstrahlung, etc) are therefore neglected. Based on these assumptions, the counts at the detector C_b should be directly proportional to the total neutron yield Y_n of a plasma discharge according to the following formula:

$$C_b = \left(K_b^n + K_b^\gamma\right) Y_n = K_b\ Y_n \tag{1}$$

where:

- K_b^n is the direct neutrons coefficient,
- K_b^γ is the prompt gamma-ray coefficient,
- K_b is the total background coefficient.

At JET, C_b was obtained from the gamma-ray detector measurements as the integrated number of events above 1 MeV and, since JET was equipped with absolutely calibrated neutron monitors, the neutron yield Y_n was provided by the JET neutron counters, therefore allowing for a direct calculation of K_b. In the case of ITER, on the other hand, only Y_n is available from simulations of various planned scenarios accessible at the IMAS [15]. The corresponding C_b must instead be inferred using an estimated K_b which, as explained later, can be extrapolated from the value obtained at JET.

Although, in principle, this coefficient could vary with the plasma emission shape or other plasma parameters, the neutron-induced background arises from interactions with the entire reactor environment, resulting in an effectively constant coefficient largely independent of the specific plasma shape or discharge conditions [23].

Regarding the direct neutrons coefficient, it can be thought of as the product of the following coefficients:

$$K_b^n = T\, A_n\, \varepsilon_n \tag{2}$$

where:

- T is the transport factor, namely the average optical probability for a particle born in a generic point inside the vessel to reach the detector,
- A_n represents the neutron attenuation factor, namely the fraction of neutrons transmitted across the neutron attenuator,
- ε_n is the lanthanum bromide detection efficiency to a neutron, which is practically unitary for a 3×3 inches crystal.

For both JET and ITER, the optical background transport factor T can be evaluated using Linalytic [14], a semi-analytical Python tool originally developed for the JET DTE2 campaign [7]. This script computes the optical paths of particles generated inside the vessel and travelling toward the detector. Its accuracy was validated against MCNP simulations, showing agreement within 1%. For JET, Linalytic applied to the same set of 89 DTE2 discharges used when developing the novel approach [7] yields an average value of $T = 2.271 \cdot 10^{-9}$. The same code used for ITER, based on the scenario set used in the previous works [17, 18], results in an estimated value of $T = 1.152 \cdot 10^{-10}$.

The attenuation factor A_n, instead, can be obtained for both JET and ITER through simple MCNP simulations [24] of the direct 14 MeV neutron transmittance across the LiH cylinder. Given the fact that the RGRS is planned to be installed and put in operation in the DT phase, we can focus on DT neutrons solely. The resulting values are $3.89 \cdot 10^{-4}$ for JET and $1.0 \cdot 10^{-7}$ for ITER. The use of a longer attenuator in ITER was specifically chosen to fully suppress the direct neutron flux. In the simulations, the neutron source was modelled as a three inches diameter disc emitting 14.1 MeV neutrons toward the detector, through the LiH barrier.

Regarding the prompt gamma-rays coefficient K_b^γ, the modelling requires the adoption of more restrictive assumptions. Specifically, only neutrons generated within the plasma and directly impinging on the vessel are considered capable of producing prompt gamma-rays (for a matter of geometrical ease, scattered neutrons are neglected); when such a neutron hits the wall, gamma-rays are emitted isotropically with a prompt gamma-ray production probability (P_{pgp}). Then, a fraction of these gamma-rays propagates toward the detector according to an optical background transport factor T_b, undergoing first attenuation by the neutron attenuator, characterized by a background transmittance A_b, and then detection with a given background gamma-ray detection efficiency ε_b. In formula, this can be summarized as:

$$K_b^\gamma = f_n\, a\, T_b\, P_{\mathrm{pgp}}\, A_b\, \varepsilon_b \tag{3}$$

where, in addition to the previously defined parameters:

- f_n is the direct neutron flux per source particle and unitary surface at the tokamak walls,
- a is the walls surface intercepted by the detector LoS.

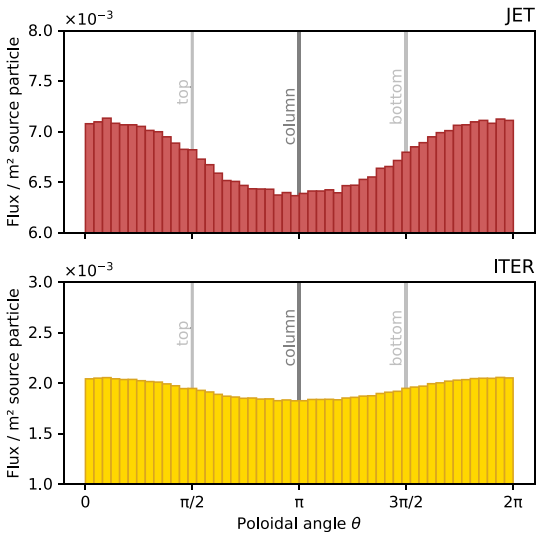

Figure 2. Neutron flux per source particle f_n expected at the in-vessel components for JET and ITER according to the performed Monte Carlo simulations with a simplified tokamak and neutron source geometry (more information in the main text). The angle $\theta = 0$ corresponds to the low field side midplane position.

All parameters (except for P_{pgp}) can be either calculated or simulated for both JET and ITER. The attenuation through the LiH attenuator can be evaluated using MCNP simulations, assuming a thickness of 90 cm for JET and 120 cm for ITER. The gamma-ray source was modelled as a disc with the same diameter as the detector (three inches), emitting radiation toward the detector. Its energy distribution was derived by deconvolving the background spectrum measured at JET. The resulting coefficients are $A_b = 0.178$ and $\varepsilon_b = 0.861$ for JET and $A_b = 0.128$ and $\varepsilon_b = 0.679$ for ITER. The difference in detection efficiency arises from the use of different detectors: a 3×6 inches detector at JET, and a 3×3 inches detector planned for ITER. The parameters f_n, a, and T_b can be estimated as described in the following subsections.

The core approach is to determine P_{pgp} from JET DTE2 data and the corresponding coefficients and then assume that this probability remains approximately valid across different machines, applying it also to ITER. Being derived not only from counts and simulations but also measurements, this P_{pgp} coefficient could be better interpreted as an effective background production probability which also includes the effect of scattered neutrons and other neglected emissions. In practice, P_{pgp} depends on the materials constituting the vessel. At JET, the relevant surface materials were primarily composed of beryllium, inconel, and copper; whereas at ITER, the central column facing components are still to be determined conclusively.

The next subsection describes the estimation of the neutron flux f_n; the following one focuses on the evaluation of the wall surface a and the optical background transport factor T_b, while the third details the determination of the prompt gamma-ray production probability P_{pgp}.

2.1. Neutron flux at the vessel

A simple Monte Carlo approach is employed to estimate the direct neutron flux f_n at the tokamak in-vessel components for both JET and ITER. Since only unscattered neutrons are considered, the method is purely geometrical. A Python script was developed for this purpose, modelling the vessel as a torus with circular cross-section, characterized by its nominal major (R) and minor (r) radii: $R = 2.96$ m and $r = 1.25$ m for JET, and $R = 6.20$ m and $r = 2.08$ m for ITER. The neutron source was modelled as a one-dimensional toroidal ring, centred in the middle of each poloidal Section, with no spatial extension in the poloidal plane, emitting isotropically in the three-dimensional space. For each emitted particle, the point of impact on the torus is computed analytically. As expected, the flux distribution results uniform along the toroidal direction, while the resulting flux distributions on the poloidal direction are shown in figure 2 for JET and ITER, normalized per source particle.

Due to the larger size of the ITER vessel, its resulting direct neutron flux is lower than in JET. Moreover, due to its lower r/R ratio, the probability distribution for ITER features reduced variations with respect to the JET case, being closer to a cylindrical approximation. Since the LoSs of both JET and RGRS detectors intersect the vessel at or close to the equatorial plane, only the flux values at toroidal

Table 1. Neutron flux per source particle f_n expected at the central column and the low field side (LFS), midplane in-vessel components for JET and ITER according to the performed simplified Monte Carlo simulations.

Tokamak	Column (m^{-2})	LFS vessel (m^2)
JET	$6.365 \cdot 10^{-3}$	$7.135 \cdot 10^{-3}$
ITER	$1.828 \cdot 10^{-3}$	$2.060 \cdot 10^{-3}$

Table 2. LoSs intercepted in-vessel components surfaces a and average optical transport factors T_b for all detectors under analysis.

Machine	Detector	Structure	$a(m^2)$	T_b
JET	—	Column	$2.208 \cdot 10^{-1}$	$4.664 \cdot 10^{-7}$
JET	—	LFS vessel	$5.438 \cdot 10^{-2}$	$3.304 \cdot 10^{-7}$
ITER	Detector 1	Column	$2.712 \cdot 10^{-2}$	$1.189 \cdot 10^{-6}$
ITER	Detector 2	Column	$2.906 \cdot 10^{-2}$	$1.131 \cdot 10^{-6}$
ITER	Detector 3	Column	$2.970 \cdot 10^{-2}$	$1.208 \cdot 10^{-6}$

angles $\theta = \pi$ (central column) and $\theta = 0$ LFS, midplane in-vessel components) are considered relevant for this study and are listed in table 1.

This simplified representation of the source and vessel geometries inevitably introduces some inaccuracy in the neutron flux calculated at the tokamak walls. To estimate the magnitude of this error, we benchmark it against an even more rudimentary approximation. By modelling the torus as a sphere and treating the plasma as a point-like neutron source at its center, the resulting neutron flux at the sphere's surface deviates by less than 7% from the values reported in table 1 for both JET and ITER. We can therefore reasonably expect the accuracy of our method to remain within the same order of magnitude.

2.2. LoS intercepted surface and particle transport

The area a of the central column or LFS in-vessel components intercepted by the detectors LoS is determined using the Linalytic code again. Instead of using it for source particles in the plasma, it is used to compute the probability for prompt gamma-rays born at the LFS vessel (or central column) to reach the detector. This can be done by discretising the surface into dense pixels and computing the optical transport probability for each of them. The non-null probability pixels contribute to the total area, leading to two distinct sets: the pixels areas $\{a_i\}$ and their transport factors $\{T_i\}$. The found total intercepted areas are listed in table 2 together with their relative weighted average transport factors T_b computed as:

$$T_b = \frac{\sum_i T_i a_i}{a} \tag{4}$$

where i runs over all surface pixels. Note that the product between T_b and a is equivalent to the sum over all pixels of the product between each pixel area and its transport probability.

In the case of the JET gamma-ray spectrometer, due to its tangential orientation, the LoS intersected both the central column and the vessel walls behind it: the two areas are summed and the transport coefficients weighted-averaged before being inserted in the main formula for K_b^γ computation. The surface on the column is four times larger than the other, being the surface smeared on the column itself. At ITER, the detectors are radially aligned, so the three LoSs intersect only the central column in approximately circular areas. In figure 3, the resulting footprint is shown for the RGRS detector 2. Compared to the JET surface on the LFS in-vessel components, the RGRS areas are smaller because the collimators are narrower. However, the transport probabilities are higher at ITER because the detectors are closer to the plasma ($\sim$ 18 m against $\sim$ 25 m).

2.3. Prompt gamma-ray probability

As previously stated, the prompt gamma-ray production probability requires prior determination of the K_b coefficient at JET. Let us recall its definition:

$$K_b = K_b^\gamma + K_b^n = \frac{C_b}{Y_n} \tag{5}$$

While the DT neutron yields Y_n are provided by JET for each plasma discharge, the background counts at the detector must be determined independently. DT plasmas also generate 2.5 MeV DD neutrons from

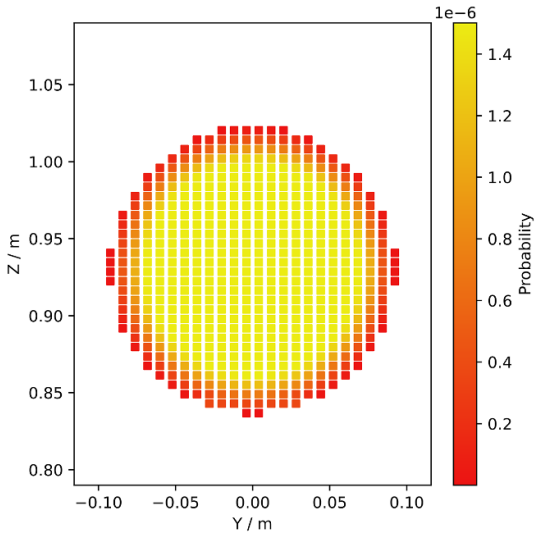

Figure 3. Central column surface intercepted by the RGRS detector 2 at ITER. The colour scheme corresponds to the optical transport probability toward the detector.

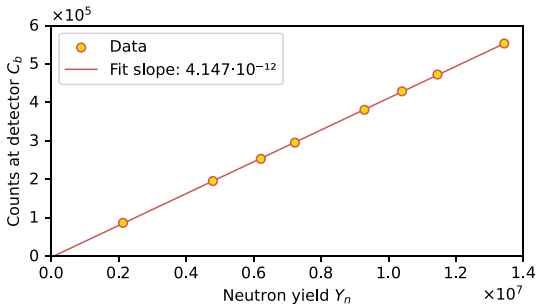

Figure 4. Integrated counts above 1 MeV acquired with the JET tangential gamma-ray spectrometer versus the corresponding neutron yield provided by JET for 7 DTE2 discharges. The fitting line slope corresponds to the K_b factor, while its y-intercept ($-3.1 \cdot 10^3$) was disregarded.

the D(D,^{3}He)n fusion reaction, which become significant when the tritium concentration in the fuel is below 3%–4%. In cases where DT neutron-induced background dominates, on the other hand, the total number of background events C_b is expected to scale linearly with the total DT neutron yield, according to K_b.

As discussed in section 1, due to a too high event rate at the scintillator, only a few DTE2 discharges with tritium content above 4.5% are suitable for the analysis. These include JET pulse numbers 99 657, 88 658, 99 659, 99 660, 99 663, 99 664, and 99 665. Above this threshold, the DD neutron contribution is assumed negligible. After subtracting the intrinsic activity of the lanthanum bromide detector, the integrated counts above 1 MeV are plotted against the neutron yield measured by the JET neutron monitors in figure 4. A linear fit is performed to extract the linear proportionality factor, resulting in $K_b = 4.147 \cdot 10^{-12}$. The y-intercept ($-3.1 \cdot 10^3$) is disregarded, as it is negligible compared to the total number of counts in the analysed spectra ($\sim 5.5 \cdot 10^5$).

With all coefficients determined, the prompt gamma-ray production probability can be calculated, yielding to $P_{\mathrm{pgp}} = 2.717 \cdot 10^{-2}$. This implies that approximately 3% of all neutrons impinging on the vessel walls result in prompt gamma-ray emission.

3. Results

Under the assumption discussed in section 2, according to which prompt gamma-ray production probability is independent of the in-vessel components material, the expected background intensity at ITER can be estimated as a function of the neutron rate using the computed P_{pgp} from JET, which leads to

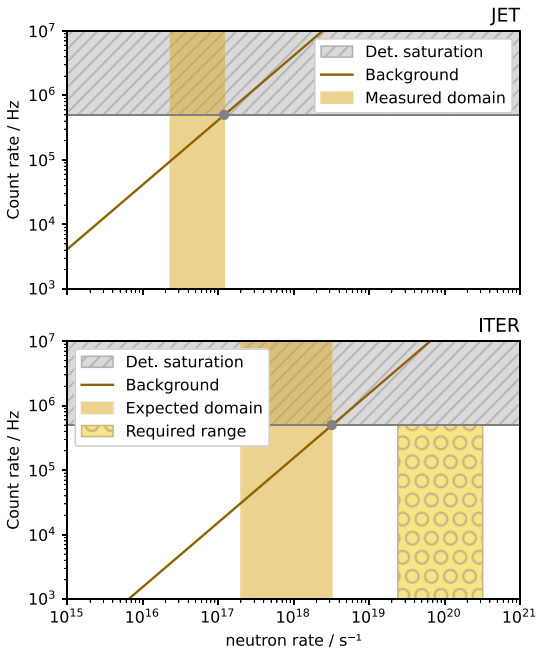

Figure 5. Operational domain of the JET tangential gamma-ray spectrometer (above) and foreseen for the ITER RGRS (below) based on the measured or predicted signal and background intensities. The background intensity is also shown as a function of the neutron rate in both plots. The requested neutron rate range for machine protection at ITER is shown in yellow the plot below.

$K_b = 1.549 \cdot 10^{-13}$ for ITER. Since the upper operational limit is determined by detector saturation due to excessive background, K_b can now be used to determine the neutron rate corresponding to the detector saturation. Based on JET data, the maximum acceptable background event rate is $C_b = 500\,\text{kHz}$. Detector 3 was used as a reference for all RGRS detectors, since its largest LoS impinging area and highest background transport probability make it the most likely to saturate first.

To fully define the operational domain, however, the lower limit must also be established. At JET, this is derived from experimental observations: the DT gamma-ray signal at the tangential spectrometer was measurable only when the total neutron yield exceeded $2.3 \cdot 10^{16}$ neutrons. For ITER, the lower limit was estimated at $2.6 \cdot 10^{17}$ $\text{n}\,\text{s}^{-1}$, as reported in [17]. Given the time resolution is fixed at 1 s per ITER requirements, no distinction is to be made between rates and yields.

The background intensity as a function of the neutron rate is shown in figure 5 for both JET and ITER, based on the K_b coefficients calculated in section 1. The figure also includes the 500 kHz upper count limit as a horizontal shaded area and the operational domains as vertical shaded areas. For the RGRS, the operational domain results between $2.6 \cdot 10^{17}$ neutrons per second and $3.2 \cdot 10^{18}$ neutrons per second. In the plot below, the requested neutron rate range is shown as a circle-filled yellow-shaded area: as can be observed, it is related only to high power plasma scenarios, from 70 to 900 MW. Given the requirements on fusion power measurements at ITER, therefore, it is now possible to notice that the foreseen RGRS operational domain has to be drifted up to match the requested neutron rate range. This can be done by including a gamma-ray attenuator in front of the detector, thus reducing both the signal and the background intensities.

At JET, the background gamma-ray spectrum spanned the low-energy range up to approximately 9 MeV, while the majority of the DT signal was concentrated between 12 and 17 MeV. The background average energy was around 4.5 MeV, compared to an average energy of about 15 MeV for the signal. This energy separation is anticipated at ITER as well, since prompt gamma-ray emissions typically exhibit a decreasing probability of producing photons with energies significantly above 9 MeV. As a consequence, this energy parting can be exploited by employing an attenuator which attenuates the background more than the signal, therefore also increasing the operational domain besides shifting it. For instance, we could require the signal to be suppressed by a factor 10 (decreasing its transmittance factor to one-tenth of the original one) and check which is the achievable transmittance on the background with different attenuator materials.

Table 3. Density (second column) and transmittance at 4 MeV (last column) for the proposed attenuator materials. The attenuators length was selected in order to provide a 10% transmittance at 15 MeV.

Material	Density g(cm^{-3})	Length (cm)	A_b
Graphite	2.2	61.64	0.016
Aluminium	2.7	38.85	0.038
Titanium	4.5	18.53	0.071
Iron	7.9	9.43	0.085
Tungsten	19	2.25	0.178

The selected attenuators should meet the following interaction criteria:

- attenuate the signal as little as possible,
- attenuate the background as much as possible,
- produce prompt gamma-rays as little as possible,
- activate as little as possible.

The most common gamma-ray attenuating materials, like heavy metals, present the drawback of attenuating more the signal than the background. Because of their high atomic number Z, in fact, the pair-production probabilities at high energies is dominant. In general, this effect becomes significant for increasing Z. Consequently, although heavy-metal attenuators were still considered, particular emphasis was placed on low-Z materials, which are typically not employed for gamma-ray attenuation.

The most promising materials are listed in table 3 together with their densities in the second column. Tungsten has been added as well for comparison. The lengths in the third column have been selected in order to provide a 10% transmittance of the signal. The last column shows the transmittance for the background at 4 MeV. The attenuation coefficients used to evaluate transmittances were taken from the NIST [25].

The achievable operational domains are shown in figure 6. The best background-to-signal attenuations also have the longest required attenuator lengths. As expected because of its high atomic number, despite being the shortest option, tungsten tightens the operational domain. Regarding all the other materials, they could not fit within the detector cassette and would require additional space inside the bio-shield penetration. Moreover, aluminium and graphite attenuators would be so long as to exceed the space available. Titanium and iron are the only options which meet the requirements, provided that a steel alloy is used in stead of iron to avoid corrosion issues.

In order to match the requested operational domain, in particular, 33 cm of titanium or 18 cm of steel (where the 136 L was selected as steel type) would be sufficient. Further investigations are ongoing in order to find the most viable solution, also considering the possibility to use different attenuators along different LoSs.

4. Discussion

The presented method allows to estimate the expected operational domain of the RGRS diagnostic at ITER for fusion power assessment. The estimate is based on extrapolations from the measurements performed at JET during the DTE2 with the tangential gamma-ray spectrometer and a series of assumptions on the measured background.

Among these, the fact that the background is due either to direct neutrons or neutron-induced prompt gamma-rays generated at the tokamak walls. At JET, the studies led to a direct neutrons factor $K_b^n = 8.834 \cdot 10^{-13}$ and a gamma-ray factor $K_b^\gamma = 3.263 \cdot 10^{-12}$. Thus, the main contribution is due to neutron-induced gamma-rays. At ITER, the neutron factor resulted in $K_b^n = 1.152 \cdot 10^{-17}$ which is completely negligible compared to the gamma-ray factor $K_b^\gamma = 1.549 \cdot 10^{-13}$. Therefore, the direct neutron flux will be fully suppressed thanks to the longer LiH neutron attenuator planned for the measurements.

Compared to that of the JET spectrometer, the RGRS operational domain will be larger and shifted to higher neutron rates. On the one hand, once normalized to the number of fusion reactions, the signal at ITER will be weaker than that at JET. The reason lies in the larger tokamak size and the detector geometry, which will have a smaller LoS diameter (3 inches at JET and 2 cm at ITER) and will roughly be located at the same distance from the plasma, thus covering a smaller portion of the total plasma

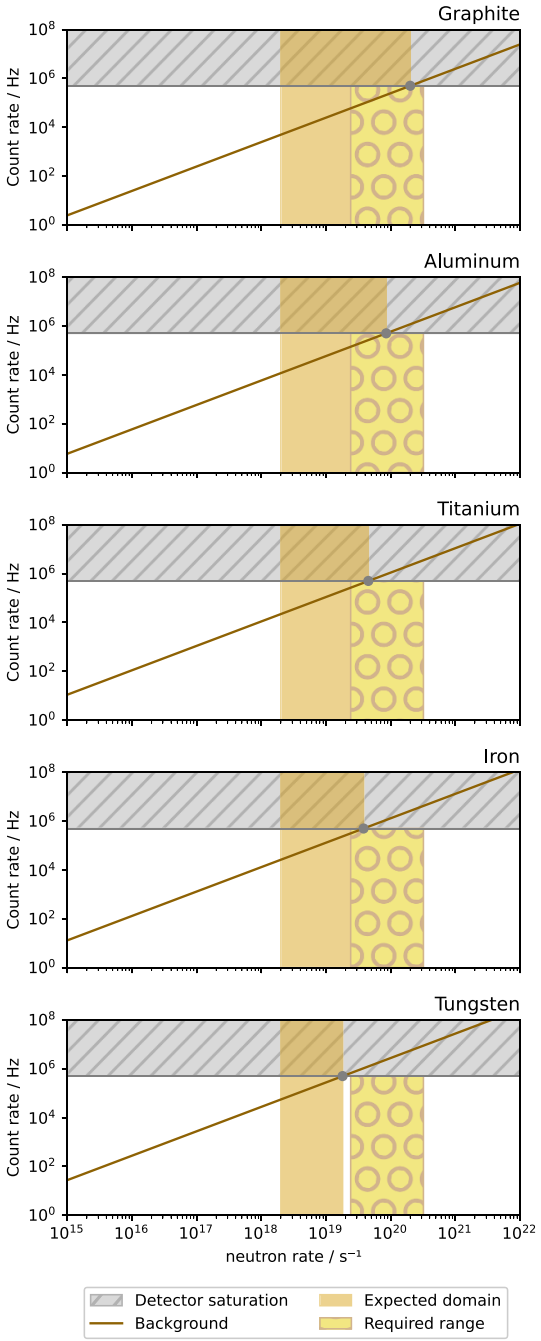

Figure 6. Modified operational domains predicted for the RGRS detector by means of different gamma-ray attenuators.

volume. In fact, the direct particles coefficient T contains this information, being larger at JET by a factor 20 ($2.271 \cdot 10^{-9}$ against $1.152 \cdot 10^{-10}$). On the other, the different geometry of the detectors LoSs will lead to an even weaker background intensity. The K_b factors, in fact, differ by almost a factor 30 (JET K_b / ITER $K_b = 26.7$), mainly because the intercepted in-vessel components surface will be smaller. This highlights the advantage of a radial LoS over a tangential one, as the latter captures radiation from the central column on a smeared area.

Based on the expected background intensity, though, the RGRS operational domain would not be suitable for ITER DT operation, since the detectors would saturate too fast. The use of gamma-ray attenuators in front of the detectors will be necessary to shift the operational domain at higher neutron rates, possibly also widening it by leveraging the difference in energy between signal and background and employ a material which attenuates low energy gamma-rays more than more energetic ones. Based on first considerations, the attenuator might consist of 33 cm of titanium or 18 cm of steel 136 L. As next

steps, the search for the most suitable gamma-ray attenuator will continue, including detailed Monte Carlo simulations of the attenuating materials effect on the signal and prompt gamma-ray spectra.

Given the obtained results, it would be interesting to point out that this observed (at JET) and expected (at ITER) proportionality between the background intensity and the total neutron yield could in principle be exploited for direct fusion power measurements too. Though, the lack of understanding of the background source processes would force it to be a relative measurement instead of an absolute one. Furthermore, any change in the environment would entail a different rescaling coefficient K_b which shall be reassessed with a dedicated calibration. Efforts will be made to describe the background quantitatively by studying all the cross sections reported in various simulation platform libraries and comparing them with each other and with the latest experiments. This would allow for reliable background simulations for ITER, which could then be benchmarked against the results of this work.

5. Conclusions

A method has been developed to estimate the background intensity expected at the ITER RGRS detectors based on extrapolations from the background intensity measured at JET with the tangential gamma-ray spectrometer during the DTE2. The method leverages a series of physical assumptions and has been used to estimate the background intensity as a function of the plasma total neutron rate, leading to the assessment of the RGRS expected operational domain.

At JET, the background was primarily due to direct neutrons or prompt gamma-rays produced through neutron interaction with the in-vessel components. In the developed method, the key parameter is the prompt gamma-ray production probability P_{pgp}, namely the probability that a gamma-ray is produced isotropically whenever a neutron impinges on the tokamak walls. This factor has been quantified at JET resulting in $P_{\mathrm{pgp}} = 2.717 \cdot 10^{-2}$ and has been assumed to be valid also for ITER. This constant has been used in a formula that describes the full prompt gamma-ray production process, starting from neutron creation in the plasma and ending with the gamma-ray detection. Each of the factors composing this formula has been estimated with light Monte Carlo simulations or numerical-analytical computations.

While this method allows for estimating the neutron rate corresponding to detectors saturation due to excessive background intensity, the lower limit of the operational domain has been inherited from two previous works [14, 17, 18]. This made it possible to determine the RGRS operational domain, resulting in neutron rates between $2.6 \cdot 10^{17}$ and $3.2 \cdot 10^{18}$ neutrons per second. However, this range is not compatible with the one requested by the ITER nuclear regulator for machine protection, which is between $2.4 \cdot 10^{19}$ and $3.2 \cdot 10^{20}$ neutrons per second. In order to make the RGRS compatible with this requirement, it must be equipped with a proper gamma-ray attenuator. Studies on the deployment of such an attenuator are still ongoing, currently leading to titanium or a steel alloy as promising materials which would allow the diagnostics to operate within the ITER fusion power measurement requirements.

The method described in this work could be extended to other future tokamaks. This would allow for synthetic diagnostic studies and performance assessments of fusion power diagnostics regarding both signal and background intensity estimations.

6. Disclaimer

The views and opinions expressed here do not necessarily reflect those of the ITER Organization.

Data availability statement

The data that support the findings of this study are available from the corresponding author upon reasonable request.

Author contributions

Giulia Marcer 0000-0002-1170-5925
Conceptualization (lead), Data curation (lead), Formal analysis (lead), Investigation (equal), Methodology (lead), Software (lead), Writing – original draft (lead), Writing – review & editing (lead)

Federico Scioscioli 0009-0007-4149-2477
Conceptualization (supporting), Investigation (supporting), Methodology (supporting), Supervision (equal), Validation (lead), Writing – review & editing (equal)

Gabriele Croci 0009-0004-3302-4209
Funding acquisition (lead), Project administration (equal), Supervision (equal)

Andrea Dal Molin 0000-0003-0471-1718
Supervision (equal), Validation (equal), Writing – review & editing (supporting)

Giuseppe Gorini 0000-0002-4673-0901
Funding acquisition (equal)

Andrea Muraro 0000-0002-4570-4576
Investigation (supporting), Methodology (supporting), Supervision (supporting)

Massimo Nocente 0000-0003-0170-5275
Conceptualization (lead), Formal analysis (supporting), Investigation (supporting), Methodology (equal), Supervision (equal)

Enrico Perelli Cippo 0000-0002-8151-3427
Investigation (supporting), Methodology (supporting), Writing – review & editing (supporting)

Marica Rebai 0000-0002-0247-9073
Funding acquisition (equal), Project administration (equal)

Davide Rigamonti 0000-0003-0183-0965
Investigation (supporting), Methodology (supporting), Supervision (supporting)

Bruno Coriton 0000-0002-0067-967X
Project administration (lead), Resources (supporting), Supervision (equal), Validation (supporting), Writing – review & editing (lead)

Andrei Kovalev 0000-0003-1784-9644
Project administration (supporting), Resources (supporting), Writing – review & editing (supporting)

Alexei Polevoi 0009-0007-9312-799X
Resources (lead), Writing – review & editing (supporting)

Marco Tardocchi 0000-0001-8443-1809
Funding acquisition (equal), Project administration (supporting), Supervision (equal)

References

[1] Gauché F and Garin P 2007 Cadarache: the site for ITER *Revue Générale Nucléaire* 80–84
[2] Jarvis O, Sadler G, Van Belle P and Elevant T 1990 In-vessel calibration of the JET neutron monitors using a ^{252}Cf neutron source: difficulties experienced *Rev. Sci. Instrum.* **61** 3172–4
[3] Nishitani T, Takeuchi H, Kondoh T, Itoh T, Kuriyama M, Ikeda Y, Iguchi T and Barnes C W 1992 Absolute calibration of the JT-60U neutron monitors using a ^{252}Cf neutron source *Rev. Sci. Instrum.* **63** 5270–8
[4] Hoek M, Nishitani T, Ikeda Y and Morioka A 1995 Neutron yield measurements by use of foil activation at JT-60U *Rev. Sci. Instrum.* **66** 885–7
[5] Bertalot L, Roquemore A, Loughlin M and Esposito B 1999 Calibration of the JET neutron activation system for DT operation *Rev. Sci. Instrum.* **70** 1137–40
[6] Marcer G *et al* 2025 Absolute measurement of the deuterium-tritium reaction gamma-ray emission in magnetic confinement fusion plasmas *Nucl. Fusion* **65** 086036
[7] Molin A D *et al* 2024 Measurement of the gamma-ray-to-neutron branching ratio for the deuterium-tritium reaction in magnetic confinement fusion plasmas *Phys. Rev. Lett.* **133** 055102
[8] Rebai M *et al* 2024 First direct measurement of the spectrum emitted by the ^{3}H(^{2}H, γ)^{5}He reaction and assessment of the relative yield Γ_1 to Γ_0 *Phys. Rev. C* **110** 014625
[9] Nocente M *et al* 2022 Fusion product measurements by nuclear diagnostics in the Joint European Torus deuterium-tritium 2 campaign *Rev. Sci. Instrum.* **93** 9

[10] Nocente M et al 2013 High resolution gamma ray spectroscopy at MHz counting rates with $LaBr_3$ scintillators for fusion plasma applications *IEEE Trans. Nucl. Sci.* **60** 1408–15
[11] Chugunov I, Shevelev A, Gin D, Naidenov V, Kiptily V, Edlington T, Syme B and the JET EFDA contributors 2008 Testing the neutron attenuator based on ^{6}LiH for γ-ray diagnostics of plasmas in the JET tokamak *Instrum. Exp. Tech.* **51** 166–70
[12] Rigamonti D et al 2022 Role of neutron attenuators for gamma-ray measurements in deuterium-tritium magnetic confinement plasmas *Rev. Sci. Instrum.* **93** 093515
[13] Colombi S et al 2026 Mcnp-based characterization of the high-energy background in gamma ray spectrometers for fusion power measurements in DT plasmas submitted
[14] Marcer G 2025 A novel method for DT fusion power measurement in magnetic confinement plasmas based on the gamma ray emission from the D(T, ^{5}He) γ reaction *PhD Thesis* (Univesity of Milano-Bicocca)
[15] Kos L et al 2017 IMAS for SOLPS-ITER *NENE 2017, React. Phys.* 712
[16] Scioscioli F et al 2025 Design and development status of the ITER radial gamma ray spectrometer *Fusion Eng. Des.* **221** 115376
[17] Marcer G et al 2024 Development of a measuring technique based on JET second DT campaign (DTE2) experience for assessing fusion power at ITER during DT operation using the radial gamma-ray spectrometer *Rev. Sci. Instrum.* **95** 8
[18] Landsmeer C et al 2025 A machine learning case study in nuclear fusion: assessment of the absolute deuterium-tritium fusion power of ITER with gamma-ray spectroscopy *Energy AI* **21** 100526
[19] Hammad M E et al 2019 Pile-up correction algorithm for high count rate gamma ray spectroscopy *Appl. Radiat. Isot.* **151** 196–206
[20] Petrovivc T et al 2014 Efficient reduction of piled-up events in gamma-ray spectrometry at high count rates *IEEE Trans. Nucl. Sci.* **61** 584–9
[21] Bolic M et al 2009 Pileup correction algorithms for very-high-count-rate gamma-ray spectrometry with NaI(Tl) detectors *IEEE Trans. Instrum. Meas.* **59** 122–30
[22] Zuo J et al 2024 High count rate gamma ray pile-up correction method of NaI(Tl) detector based on deconvolution method *Nucl. Instrum. Methods Phys. Res. A* **1061** 169135
[23] Marcer G et al 2021 Study of a single line of sight gamma ray diagnostics for measurements of the absolute gamma ray emission from JET *J. Instrum.* **16** C12019
[24] Rising M E et al 2023 MCNP® code version 6.3.0 release notes *Technical Report LA-UR-22-33103*
[25] NIST x-ray mass attenuation coefficients (available at: https://physics.nist.gov/PhysRefData/XrayMassCoef/tab3.html)